Transient Analysis of Coupled Transmission Lines Using Scattering Parameter Based Macromodel

Jimmy Shinn-Hwa Wang
Dr. Wayne Wei-Ming Dai

UCSC-CRL-94-09
11 April 1994

Baskin Center for
Computer Engineering & Information Sciences
University of California, Santa Cruz
Santa Cruz, CA 95064 USA

ABSTRACT

As the system clock speed increases, crosstalk becomes one of the major sources of noise which can limit the performance of high-speed digital systems in addition to delay and ringing. The congruence transformation can be used to decouple a coupled transmission-line system. In this paper, we extended the scattering parameter based macromodel to include the congruence transformation to analyze the crosstalk in the coupled transmission-line systems. After decouple the n coupled transmission lines using the congruence transformation, the computation of scattering matrix of the coupled transmission lines then becomes those of the scattering matrix of the congruence transformers and those of the n decoupled single transmission lines. A very simple scattering parameter description of the congruence transformer for coupled lossless transmission lines is derived. It has been extended to handle the coupled lossy transmission lines. Unlike some of the previous methods[14][16] which only consider the coupling between immediate adjacent lines, our method takes into account the coupling among all lines. We also present the results obtained from our simulator as well as those obtained from the SPICE-like simulators (for example: SPICE3e2 and ASTAP) and state- of-the-art moment-matching simulators (for example: SWEC and Coffee).

Keywords: Coupled Transmission Lines, Transient Analysis, Congruence Transformation, Scattering Parameters, Macromodel, S-Parameter Based Simulator.

Contents

1 Introduction

As the system clock speed increases, crosstalk becomes one of the major source of noise in addition to the delay and ringing which can limit the performance of high-speed digital systems [2] [3] [5] [6] [7] [14] [15] [16]. The crosstalk can often lead to excessive overshoots, undershoots and glitches. It can also cause false switchings on the non-active lines as well as undetected switchings on the active lines, not to mention that it can also increase power dissipation of the output drivers. It can be considered as the dominant factor of noise in the high density interconnection networks. Thus for a reliable operation, the crosstalk should be strictly controlled within a certain limit. An efficient and accurate transient analysis also becomes a key element in the combating of the crosstalk.

Previous research works which uses scattering parameter for the analysis of coupled transmission lines include those of the full-wave analysis by Cooke et al [6] and time domain simulation by Schutt-Aine et al [16]. In Schutt-Aine's paper, they demonstrated a great accuracy improvement in simulating circuits that includes non-linear drivers and terminations [16]. Whereas in Cooke's paper, they illustrated an ability to simulate frequency dependent model propagation [6]. Recently, a frequency domain simulator using scattering parameter based macromodels has been presented by Liao et al [11] [12]. Based on the scattering parameter based macromodel, Pade technique or Exponentially Decayed Polynomial Function (EDPF) can be used to approximate transfer functions of the coupled interconnects. This approach avoids the costly matrix computation for converting the frequency domain scattering parameter matrix representation into the time domain transfer/reflection matrix representation [16] and the time consuming full-wave analysis [6]. An adoption of the scattering parameter based macromodel and Pade/EDPF approximation do provide a trade off between speed and accuracy.

The difficulty in high-performance system design comes from the coupled noise among the transmission lines which are placed closely together in today's dense process technology. The coupled noise (crosstalk) is inversely proportion to the interline spacing and is proportional to

several parameters including those of the thickness of the dielectric material, the distance which the coupled lines are in parallel, the rate of change of the input waveforms, and the line impedances. There are signal distortions caused by coupling mechanisms such as n mode propagation and crosstalk. In order to rigorously analyze crosstalk in a coupled transmission line systems, the method of congruence transformation decoupling can be employed [2] [3] [9] [14]. The analysis is focused on finding the crosstalk among all of the possible coupling lines, but not limited to the immediate adjacent lines. The scattering parameter based macromodel provides the crucial information about the crosstalk waveforms for the coupled transmission lines analysis and design.

In Section 2, the congruence transformation of lossless coupled transmission lines is derived based on frequency-independent per-unit-length $\mathbf{L}$ and $\mathbf{C}$ matrices. The scattering parameter based macromodel of lossless coupled transmission lines is derived from the congruence transformation. An addition simplification of the scattering parameter based macromodel is derived based on the similarity transformation property. In Section 3, the derivation is repeated for coupled lossy transmission lines. In Section 4, several examples of lossless as well as lossy coupled transmission lines are simulated, and their results are compared with published results, commercial tools, and state-of-the-art simulators such as SWEC [13] and Coffee [4]. Finally we will conclude this paper with some remarks on the proposed method and directions for the future research.

2 Congruence Transformation of the Lossless Coupled Transmission Lines

Wave propagation in multiconductor has been extensively studied by the Microwave, Electronic-Magnetic-Compatibility (EMC), and Electrical engineers. Due to the coupling between transmission lines, different modes which have different propagation velocities exist simultaneously in the system. For an n conductor system shown in Figure 2.1, there are n fundamental modes of propagation.

Starting with the quasi-TEM analysis, the congruence transformation decoupling for the coupled lossless transmission lines can first be derived. Later based on the congruence transformation

where $0 \leq x \leq l$ and $\mathbf{v}(x,t)$ and $\mathbf{i}(x,t)$ are column vectors defining the voltages $v_k(x,t)$ and currents $i_k(x,t)$ distributed on the conductors $k = 1,2,3,...,n$. The $\mathbf{L}$ and $\mathbf{C}$ are the n by n symmetric matrices of the per-unit-length inductance and capacitance of the n conductor system. Throughout this paper, the $\mathbf{L}$ and $\mathbf{C}$ matrices are assumed to be *frequency-independent.*

2.2 Congruence Transformation of the Coupled Lossless Transmission Lines

Taking derivative with respect to x for both sides of Equation (2.1) and (2.2) with proper substitution of terms, one obtains the following equations:

$$\frac{\partial^2 \mathbf{v}(x,t)}{\partial x^2} = \mathbf{LC}\frac{\partial^2 \mathbf{v}(x,t)}{\partial t^2} \tag{2.3}$$

$$\frac{\partial^2 \mathbf{i}(x,t)}{\partial x^2} = \mathbf{CL}\frac{\partial^2 \mathbf{i}(x,t)}{\partial t^2}, \tag{2.4}$$

In order to decouple the coupled system, all four matrices $\mathbf{L}$, $\mathbf{C}$, $\mathbf{LC}$, and $\mathbf{CL}$ in Equation (2.1), (2.2), (2.3), and (2.4), must be simultaneously diagonalized.

By applying congruence transformation, we can change the variable basis from v to u and from i to j. The terminal voltages and currents at opposite sides of the transformer are related by (see Figure 2.2) [2]:

$$v_k(x,t) = \sum_{m=1}^{n} X_{km} u_m(x,t) \tag{2.5}$$

$$j_k(x,t) = -\sum_{m=1}^{n} X_{mk} i_m(x,t), \tag{2.6}$$

The negative sign is used to indicate the direction of current j_k is flowing into the transformer. Rewrite Equation (2.5) and (2.6) in a matrix notation, one obtains:

$$V(x,t) = XU(x,t) \tag{2.7}$$

$$I(x,t) = -\left(X^t\right)^{-1} J(x,t), \tag{2.8}$$

where V, U, I and J are column vectors, $V = [v_1(x,t), ..., v_n(x,t)]^t$, $U = [u_1(x,t), ..., u_n(x,t)]^t$, $I = [i_1(x,t), ..., i_n(x,t)]^t$, and $J = [j_1(x,t), ..., j_n(x,t)]^t$.

Substituting Equation (2.7) and (2.8) into Equations (2.1), (2.2), (2.3), and (2.4), one obtains:

$$\frac{\partial \mathbf{u}(x,t)}{\partial x} = -X^{-1}\mathbf{L}\left(X^t\right)^{-1}\left[-\frac{\partial \mathbf{j}(x,t)}{\partial t}\right] \tag{2.9}$$

$$-\frac{\partial \mathbf{j}(x,t)}{\partial x} = -X^t\mathbf{C}X\frac{\partial \mathbf{u}(x,t)}{\partial t} \tag{2.10}$$

$$\frac{\partial^2 \mathbf{u}(x,t)}{\partial x^2} = X^{-1}\mathbf{L}\mathbf{C}X\frac{\partial^2 \mathbf{u}(x,t)}{\partial t^2} \tag{2.11}$$

$$\frac{\partial^2 \mathbf{j}(x,t)}{\partial x^2} = X^t\mathbf{C}\mathbf{L}\left(X^t\right)^{-1}\frac{\partial^2 \mathbf{j}(x,t)}{\partial t^2}. \tag{2.12}$$

It has been shown that the right eigenvector matrix X which is obtained from the similarity transformation of $\mathbf{L}$ satisfys the following property [14]:

$$X^t = X^{-1}. \tag{2.13}$$

So the right eigenvector matrix X can simultaneously diagonalize all four matrices:

$$\tilde{\mathbf{L}} = X^{-1}\mathbf{L}\left(X^t\right)^{-1} = X^{-1}\mathbf{L}X = diag(L_k) \tag{2.14}$$

$$\tilde{\mathbf{C}} = X^t\mathbf{C}X = X^t\mathbf{C}\left(X^t\right)^{-1} = diag(C_k) \tag{2.15}$$

$$\tilde{\mathbf{L}}\tilde{\mathbf{C}} = X^{-1}\mathbf{L}\mathbf{C}X = X^{-1}\mathbf{L}\left(X^t\right)^{-1}X^t\mathbf{C}X = diag((LC)_k) \tag{2.16}$$

$$\tilde{\mathbf{C}}\tilde{\mathbf{L}} = X^t\mathbf{C}\mathbf{L}\left(X^t\right)^{-1} = X^t\mathbf{C}XX^{-1}\mathbf{L}\left(X^t\right)^{-1} = diag((CL)_k), \tag{2.17}$$

where $k = 1...n$ and $diag(L_k)$ represents an n by n diagonal matrix L which all off-diagonal elements are equal to zero. The L_k, C_k, $(LC)_k$, and $(CL)_k$ are the $k-th$ eigenvalue of the matrices $\mathbf{L}$, $\mathbf{C}$, $\mathbf{LC}$, and $\mathbf{CL}$.

Redefine the Telegraphist Equations of decoupled system to be:

$$\frac{\partial \mathbf{u}(x,t)}{\partial x} \equiv -\tilde{\mathbf{L}}\left[-\frac{\partial \mathbf{j}(x,t)}{\partial t}\right] \tag{2.18}$$

macromodel simulator. The scattering parameter based macromodel simulator takes full advantage of being a frequency domain simulator and lumps the multiport components together using the Pade or EDPF approximation [11] [12]. The derivations of equations of the voltage scattering parameter matrices of all the components in the decoupled system are presented in the next two section.

2.3 Scattering Parameter Matrix of a Congruence Transformer

Due to the choice of identical reference impedance Z_0 at any port for the scattering parameter based macromodel simulator, the scattering parameter matrix S of any multi-port component is equivalent to its voltage scattering parameter matrix S^V. Since only the terminal voltages and currents are of an interest, the following representations are introduced (see Figure 2.1):

$$v_{1k}(t) \equiv v_k(x=0,t) \quad v_{2k}(t) \equiv v_k(x=l,t) \quad i_{1k}(t) \equiv i_k(x=0,t) \quad i_{2k}(t) \equiv i_k(x=l,t),$$

where $k = 1...n$. The u_{1k}, u_{2k}, j_{1k}, and j_{2k} are the terminal voltages and currents after the transformation, they represent:

$$u_{1k}(t) \equiv u_k(x=0,t) \quad u_{2k}(t) \equiv u_k(x=l,t) \quad j_{1k}(t) \equiv j_k(x=0,t) \quad j_{2k}(t) \equiv j_k(x=l,t),$$

To find the voltage scattering parameter matrix of a congruence transformer, first the time-domain voltage and current are transformed into frequency-domain using Laplace transform. For example, $j_{pk}(s) = \mathcal{L}(j_{pk}(t))$, where $p = 1, 2$ and $k = 1, ..., n$. Then the terminal voltages and currents of the both sides of the transformer are separated into the *incident* and *reflect* wave components as shown in Figure 2.3: Writing the voltage and current wave components in vector notation, one obtains:

$$V_p = V_p^+ + V_p^- \tag{2.22}$$

$$U_p = U_p^+ + U_p^- \tag{2.23}$$

$$I_p = I_p^+ - I_p^- \tag{2.24}$$

Figure 2.3: The separatri

The definitions of voltage scattering parameters matrix S^V and its submatrices S_{11}^V, S_{12}^V, S_{21}^V, and S_{22}^V are:

$$\begin{aligned}
S^V &= \begin{bmatrix} S_{11}^V & S_{12}^V \\ S_{21}^V & S_{22}^V \end{bmatrix} \\
S_{11}^V &= \left.\frac{V_p^-}{V_p^+}\right|_{U_p^+=\mathbf{0}} \\
S_{12}^V &= \left.\frac{V_p^-}{U_p^+}\right|_{V_p^+=\mathbf{0}} \\
S_{21}^V &= \left.\frac{U_p^-}{V_p^+}\right|_{U_p^+=\mathbf{0}} \\
S_{22}^V &= \left.\frac{U_p^-}{U_p^+}\right|_{V_p^+=\mathbf{0}}
\end{aligned}$$

By arithmetic manipulation of Equations (2.22), (2.23), (2.24), (2.25), (2.26), (2.27), (2.28), (2.29), (2.30), and (2.31), and by setting U_p^+ to be an all-zero column vector, one can find S_{11}^V as:

$$S_{11}^V = -[X^{-1} + X^t]^{-1}[X^{-1} - X^t]. \tag{2.32}$$

Similarly one can find other submatrices of S^V:

$$S_{12}^V = 2[X^{-1} + X^t]^{-1} \tag{2.33}$$

$$S_{21}^V = 2[X + (X^t)^{-1}]^{-1} \tag{2.34}$$

$$S_{22}^V = -[X + (X^t)^{-1}]^{-1}[X - (X^t)^{-1}]. \tag{2.35}$$

The voltage scattering parameter matrix S^V is:

$$S^V = \begin{bmatrix} -[X^{-1} + X^t]^{-1}[X^{-1} - X^t] & 2[X^{-1} + X^t]^{-1} \\ 2[X + (X^t)^{-1}]^{-1} & -[X + (X^t)^{-1}]^{-1}[X - (X^t)^{-1}] \end{bmatrix} \tag{2.36}$$

Since the similarity transformation property $X^{-1} = X^t$ holds for all X that simultaneously

diagonalize the **L**, **C**, **LC**, and **CL** matrices, Now the scattering parameter matrix S can be simplified to:

$$S = \begin{bmatrix} 0 & X \\ X^t & 0 \end{bmatrix}. \tag{2.37}$$

This equation holds when the right eigenvector matrix X is obtained either from similarity transformation of a full **L** matrix, or Romeo's method which deals with a tri-diagonal **L** matrix.

Bayard first outlines the transformation, $\mathbf{A}^t\mathbf{Z}\mathbf{A}$, and calls it "translator" [1]. Hazony is the first one to name the transformation "congruence transformer" in his book [9]. Chang uses the congruence transformer to decouple both the lossless [2] and lossy coupled transmission lines [3]. Chang's method for the analysis of coupled lossless transmission lines relies on simultaneously diagonalizing the **L**, **C**, **LC**, and **CL** matrices using special conditioned matrix. Romeo and Santomauro present a different method of finding the right eigenvector matrices for coupled lossless transmission lines with tri-diagonal **L** and **C** matrices [14]. In this paper, one will find the right eigenvector matrices of a full **L** matrix. The method proposed here may be more preferred than Chang's method because it leads to simpler equations for scattering parameter based macromodel representation of congruence transformer. In Chang's method where the similarity transformation property $X^{-1} = X^t$ may not hold, the scattering parameter matrix representation cannot be simplified to Equation (2.37). The proposed method in more general than Romeo's method because it does not have the limitation that each transmission line is only coupled to the immediate adjacent lines.

For each of the decoupled lossless transmission line shown in Figure 2.2, its scattering parameter matrix is [8]:

$$[S] = \left[S^V\right] = \frac{1}{2Z_0Z_c\cosh(\gamma) + (Z_0^2 + Z_c^2)\sinh(\gamma)} \begin{bmatrix} (Z_0^2 - Z_c^2)\sinh(\gamma) & 2Z_0Z_c \\ 2Z_0Z_c & (Z_0^2 - Z_c^2)\sinh(\gamma) \end{bmatrix} \tag{2.38}$$

where Z_0 is the reference impedance, and both Z_c and γ are computed from the eigenvalues L_k

and C_k of the $\mathbf{L}$ and $\mathbf{C}$ matrices respectively. The $Z_c = \sqrt{\frac{L_k}{C_k}}$ is the characteristic impedance of the $k-th$ line and $k = 1...n$, and $\gamma = s\sqrt{L_k C_k} \cdot l$ is the propagation constant of the $k-th$ line and l is the coupling length.

3 Congruence Transformation of the Lossy Coupled Transmission Lines

When the ohmic loss of the conductors is not negligible, the transmission lines are considered to be lossy. It is very common that the lossy conductors are fabricated by embedding them in several layers of homogeneous dielectrical media. This structure supports TEM waves traveling at multiple propagation speeds. However, there is an attenuation in addition to phase shift that must be considered when the different modes of wave propagate through the lossy media. The decoupling analysis is repeated here for the coupled lossy transmission lines similar to the analysis done in previous section.

3.1 Quasi-TEM Wave Propagation on the Coupled Lossy Transmission Lines

With the assumption of quasi-TEM wave propagation, the distributions of voltages and currents in an n coupled lossy transmission-line system can be described by the generalized Telegraphist's equations [3]:

$$\frac{\partial \mathbf{v}(x,t)}{\partial x} = -\mathbf{L}\frac{\partial \mathbf{i}(x,t)}{\partial t} - \mathbf{R}\mathbf{i}(x,t) \tag{3.1}$$

$$\frac{\partial \mathbf{i}(x,t)}{\partial x} = -\mathbf{C}\frac{\partial \mathbf{v}(x,t)}{\partial t}, \tag{3.2}$$

where $0 \leq x \leq l$, and $\mathbf{v}(x,t)$ and $\mathbf{i}(x,t)$ are column vectors defining the voltages $v_k(x,t)$ and currents $i_k(x,t)$ distributed on the conductors $k = 1, 2, 3, ..., n$. The $\mathbf{L}$ and $\mathbf{C}$ are the n by n symmetric matrices of the per-unit-length inductance and capacitance of the n conductor system. The $\mathbf{R} = diag(R_{kk})$, $k = 1...n$ is the diagonal matrix of the per-unit-length resistance of the n conductors.

3.2 Congruence Transformation of the Coupled Lossy Transmission Lines

Chang proposes the method of congruence transformation of n coupled lossy transmission lines in his 1989 paper [3]. Taking derivative with respect to x for both sides of Equation (3.1) and (3.2) with proper substitution of terms, one obtains the following equations:

$$\frac{\partial^2 \mathbf{v}(x,t)}{\partial x^2} = \mathbf{LC}\frac{\partial^2 \mathbf{v}(x,t)}{\partial t^2} + \mathbf{RC}\frac{\partial \mathbf{v}(x,t)}{\partial t} \tag{3.3}$$

$$\frac{\partial^2 \mathbf{i}(x,t)}{\partial x^2} = \mathbf{CL}\frac{\partial^2 \mathbf{i}(x,t)}{\partial t^2} + \mathbf{CR}\frac{\partial \mathbf{i}(x,t)}{\partial t}, \tag{3.4}$$

In order to decouple the coupled system, all seven matrices **R**, **L**, **C**, **LC**, **CL**, **RC**, and **CR** must be simultaneously diagonalized.

It has been shown that the following steps can achieve this goal [3]:

1. Construct the time constant matrix **T**.
2. Find the eigenvalues of the matrix **T**.
3. Construct the congruence transformation matrix X.
4. Diagonalize all matrices using matrix X.
5. Build the decoupled system based on the diagonalized matrices.

First, one needs to find the right eigenvector matrix W of the time constant matrix **T** using standard mathematical methods such as Givens and Household method. Define the eigenvalues of time constant matrix **T** to be τ_k, one obtains:

$$\mathbf{T} \equiv \mathbf{R}^{-1/2}\mathbf{L}\mathbf{R}^{-1/2} = W diag(\tau_k) W^{-1}, \tag{3.5}$$

where $\mathbf{R}^{-1/2} = diag(1/\sqrt{R_{kk}})$, $k = 1, ..., n$, and the right eigenvector matrix W has the property of the similarity transformation $W^{-1} = W^t$.

Now applying the linear transformation:

$$V_p(t) = X U_p(t) \tag{3.6}$$

$$I_p(t) \quad = \quad -\left(X^t\right)^{-1} J_p(t), \tag{3.7}$$

where the congruence transformer matrix X is defined as:

$$X \quad \equiv \quad diag(\sqrt{R_{kk}})W diag(\sqrt{\tau_k/L_k}), \tag{3.8}$$

into Equation (3.1), (3.2), (3.3) and (3.4), after rearrangement, after rearrangements, one obtains the following Equations (3.9) to (3.12):

$$\frac{\partial \mathbf{u}(x,t)}{\partial x} = -X^{-1}\mathbf{L}\left(X^t\right)^{-1}\left[-\frac{\partial \mathbf{j}(x,t)}{\partial t}\right] - X^{-1}\mathbf{R}\left(X^t\right)^{-1}[-\mathbf{j}(x,t)] \tag{3.9}$$

$$-\frac{\partial \mathbf{j}(x,t)}{\partial x} = -X^t\mathbf{C}X\frac{\partial \mathbf{u}(x,t)}{\partial t} \tag{3.10}$$

$$\frac{\partial^2 \mathbf{u}(x,t)}{\partial x^2} = X^{-1}\mathbf{L}\mathbf{C}X\frac{\partial^2 \mathbf{u}(x,t)}{\partial t^2} + X^{-1}\mathbf{R}\mathbf{C}X\frac{\partial \mathbf{u}(x,t)}{\partial t} \tag{3.11}$$

$$\frac{\partial^2 \mathbf{j}(x,t)}{\partial x^2} = X^t\mathbf{C}\mathbf{L}\left(X^t\right)^{-1}\frac{\partial^2 \mathbf{j}(x,t)}{\partial t^2} + X^t\mathbf{C}\mathbf{R}\left(X^t\right)^{-1}\frac{\partial \mathbf{j}(x,t)}{\partial t}. \tag{3.12}$$

It can be shown that the coefficient matrices are all diagonal matrices as represented by Equations (3.13) to (3.13):

$$\begin{aligned}
\tilde{\mathbf{R}} &= X^{-1}\mathbf{R}(X^t)^{-1} = diag(R_k) = diag(L_k/\tau_k) \\
\tilde{\mathbf{L}} &= X^{-1}\mathbf{L}(X^t)^{-1} = diag(L_k) \\
\tilde{\mathbf{C}} &= X^t\mathbf{C}X = diag(C_k) = diag(1/\nu^2 L_k) \\
\tilde{\mathbf{L}}\tilde{\mathbf{C}} &= X^{-1}\mathbf{L}\mathbf{C}X = X^{-1}\mathbf{L}\left(X^t\right)^{-1}X^t\mathbf{C}X = diag(LC_k) = diag(1/\nu^2) \\
\tilde{\mathbf{C}}\tilde{\mathbf{L}} &= X^t\mathbf{C}\mathbf{L}\left(X^t\right)^{-1} = X^t\mathbf{C}XX^{-1}\mathbf{L}\left(X^t\right)^{-1} = diag(CL_k) = diag(1/\nu^2) \\
\tilde{\mathbf{R}}\tilde{\mathbf{C}} &= X^{-1}\mathbf{R}\mathbf{C}X = X^{-1}\mathbf{R}\left(X^t\right)^{-1}X^t\mathbf{C}X = diag(RC_k) \\
\tilde{\mathbf{C}}\tilde{\mathbf{R}} &= X^t\mathbf{C}\mathbf{R}\left(X^t\right)^{-1} = X^t\mathbf{C}XX^{-1}\mathbf{R}\left(X^t\right)^{-1} = diag(CR_k).
\end{aligned}$$

where $k = 1...n$ and $diag(L_k)$ represents an n by n diagonal matrix L which all off-diagonal elements are equal to zero. The R_k, L_k, C_k, $(LC)_k$, $(CL)_k$, $(RC)_k$, and $(CR)_k$ are the $k-th$ eigenvalue of

exception of X where X is now defined in Equation (3.8).

$$S = \begin{bmatrix} -[X^{-1} + X^t]^{-1}[X^{-1} - X^t] & 2[X^{-1} + X^t]^{-1} \\ 2[X + (X^t)^{-1}]^{-1} & -[X + (X^t)^{-1}]^{-1}[X - (X^t)^{-1}] \end{bmatrix}. \quad (3.17)$$

For each of the decoupled lossy transmission line shown in Figure 3.1, the scattering parameter matrix representation is the same and the computation of Z_c and γ are different [8]:

$$[S] = \left[S^V\right] = \frac{1}{2Z_0 Z_c \cosh(\gamma) + (Z_0^2 + Z_c^2)\sinh(\gamma)} \begin{bmatrix} (Z_0^2 - Z_c^2)\sinh(\gamma) & 2Z_0 Z_c \\ 2Z_0 Z_c & (Z_0^2 - Z_c^2)\sinh(\gamma) \end{bmatrix} \quad (3.18)$$

where Z_0 is the reference impedance, and both Z_c and γ are computed from the eigenvalues R_k, L_k, and C_k obtained from the diagonalization of the **R**, **L**, and **C** matrices respectively. The $Z_c = \sqrt{\frac{R_k + sL_k}{sC_k}}$ is the characteristic impedance of the $k-th$ line where $k = 1...n$, and $\gamma = \sqrt{(R_k + sL_k)(sC_k)} \cdot l$ is the propagation constant of the $k-th$ line where l is the coupling length.

4 Experiment Results

The examples presented here are some of the MCMC-94 Benchmarks (1994 IEEE Multi-Chip Module Conference Interconnect Simulation Benchmarks). The results are compared with digitized waveforms extracted from the published papers with the exception of Example 2 which instead is compared to Ansoft's Maxwell/Spicelink results. Example 3 is a coupled lossy transmission-line systems whereas the rest of the examples are coupled lossless transmission-line systems. All of the Far-end waveforms are simulated with time-of-flight captured explicitly [10]. The running time reported in all examples using our simulator or SPICE-like simulator are the running time on a SUN SPARC station 1+. The running time of other simulators are not listed because they are executed on different machines.

4.1 Example 1

The circuit and geometry parameters of Example 1 as shown in Figure 4.1 (a) is taken from Chang's paper [2]. The geometry parameters are listed in the circuit schematic with all three transmission lines are uniform in geometry. The **C** and **L** of the configuration are:

$$L = \begin{bmatrix} 3.8790\ nH/cm & 1.6238\ nH/cm & 0.8252\ nH/cm \\ 1.6238\ nH/cm & 3.7129\ nH/cm & 1.6238\ nH/cm \\ 0.8252\ nH/cm & 1.6238\ nH/cm & 3.8790\ nH/cm \end{bmatrix}$$

$$C = \begin{bmatrix} 1.0413\ pF/cm & -0.3432\ pF/cm & -0.0140\ pF/cm \\ -0.3432\ pF/cm & 1.1987\ pF/cm & -0.3432\ pF/cm \\ -0.0140\ pF/cm & -0.3432\ pF/cm & 1.0413\ pF/cm \end{bmatrix}$$

The simulation waveforms of this example are compared to Chang's and are shown in Figure 4.1 (b), (c), (d), (e), (f), and (g). The total running time for this example is 3.48 seconds. Our simulation results does not match the published measurement results too well because the extreme long time-of-flight. This kind of coupled lossless transmission line systems are best handled in time-domain using Method of Characteristic model [2].

4.2 Example 2

The circuit and geometry parameters of Example 2 as shown in Figure 4.2 (a) are taken from Romeo et al paper [14]. The **C** and **L** matrices are generated using Maxwell from Ansoft whereas the SPICE simulation results are obtained from Spicelink which uses a method derived from Djordjevic [7]. The relative permittivity is changed from 4.65 to 10.0. The geometry parameters are listed in the circuit schematic where all three transmission lines are uniform. The **C** and **L** of the configuration obtained from Maxwell are:

West-End Active Line
Volt
1.00
0.99

$$L = \begin{bmatrix} 4.9693\ nH/cm & 1.1697\ nH/cm & 0.4952\ nH/cm \\ 1.1697\ nH/cm & 4.9946\ nH/cm & 1.1691\ nH/cm \\ 0.4952\ nH/cm & 1.1691\ nH/cm & 4.9735\ nH/cm \end{bmatrix}$$

$$C = \begin{bmatrix} 1.3341\ pF/cm & -0.13852\ pF/cm & -0.010318\ pF/cm \\ -0.13852\ pF/cm & 1.33445\ pF/cm & -0.13699\ pF/cm \\ -0.010318\ pF/cm & -0.13699\ pF/cm & 1.32823\ pF/cm \end{bmatrix}$$

The simulation waveforms of this example are compared to those generated by SWEC [13], Coffee [4], and Spicelink and are shown in Figure 4.2 (b), (c), (d), and (e). All the simulation results from four different simulators agree with each other very well. The total running time of this example is 1.10 seconds. The total simulation time for Ansoft Spicelink is 7.95 seconds.

4.3 Example 3

The circuit and geometry parameters of Example 3 as shown in Figure 4.3 (a) are taken from Schutt-Aine et al paper [16]. The geometry parameters are listed in the circuit schematic where all three transmission lines are uniform. The length of this coupled system is 25 inch. The **R**, **L** and **C** of the configuration are listed as follow:

$$R = \begin{bmatrix} 0.5000\ ohm/cm & 0.0000\ ohm/cm \\ 0.0000\ ohm/cm & 0.5000\ ohm/cm \end{bmatrix}$$

$$L = \begin{bmatrix} 3.1200\ nH/cm & 1.0000\ nH/cm \\ 1.0000\ nH/cm & 3.1200\ nH/cm \end{bmatrix}$$

$$C = \begin{bmatrix} 1.0840\ pF/cm & -0.1940\ pF/cm \\ -0.1940\ pF/cm & 1.0840\ pF/cm \end{bmatrix}$$

The simulation waveforms of this example are shown in Figure 4.3 (b), (c), (d), and (e). Results from SPICE3e2 and Schutt-Aine are also plotted for comparison. The SPICE3e2 results are obtains by

applying the decoupling technique in time-domain. For all the waveform plots, our method obtains results that match SPICE3e2 simulation results better than Schutt-Aine's. The total running time for this example is 4.4 seconds.

4.4 Example 4

The circuit and geometry parameters of Example 4 as shown in Figure 4.4 are taken from Cooke's paper [6]. The driving signal is 100-MHz 50% duty-cycle pulse with $0.1ns$ rise/fall time. The estimated harmonic bandwidth of this driving signal is well over 3.5-GHz. The geometry parameters are listed in the circuit schematic where all six transmission lines are uniform. The **R**, **L** and **C** of the configuration are:

$$L = \begin{bmatrix} 5.033\ nH/cm & 1.734\ nH/cm & 0.818\ nH/cm \\ 1.734\ nH/cm & 4.972\ nH/cm & 1.734\ nH/cm \\ 0.818\ nH/cm & 1.734\ nH/cm & 5.033\ nH/cm \end{bmatrix}$$

$$C = \begin{bmatrix} 0.667\ pF/cm & -0.163\ pF/cm & -0.0145\ pF/cm \\ -0.163\ pF/cm & 0.722\ pF/cm & -0.163\ pF/cm \\ -0.0145\ pF/cm & -0.163\ pF/cm & 0.667\ pF/cm \end{bmatrix}$$

The simulation waveforms of this example are shown in Figure 4.5 (a), (b), (c), and (d). Two zoom in portion of the simulation waveforms are shown in Figure 4.5 (e) and (f). The ASTAP and Cooke's simulation waveforms are digitized from the results published in Cooke's paper [6] while the SWEC results are obtained from MCMC-94 benchmarks. The SWEC uses analytic method to find the derivatives of the admittance in order to compute the moments; because of the complexity, it only find lower order moments [13]. In all the plots, the results obtained from SWEC and our macromodel simulator agree with published ASTAP results. However, the macromodel simulation waveforms match those of the ASTAP simulator better than those derived from the SWEC. In all the waveform plots, Cooke's results deviate from the ASTAP results the most. Our method is better than Cooke's scattering parameter approach because our results match those of the ASTAP

Figure 4.4: Two Crowb

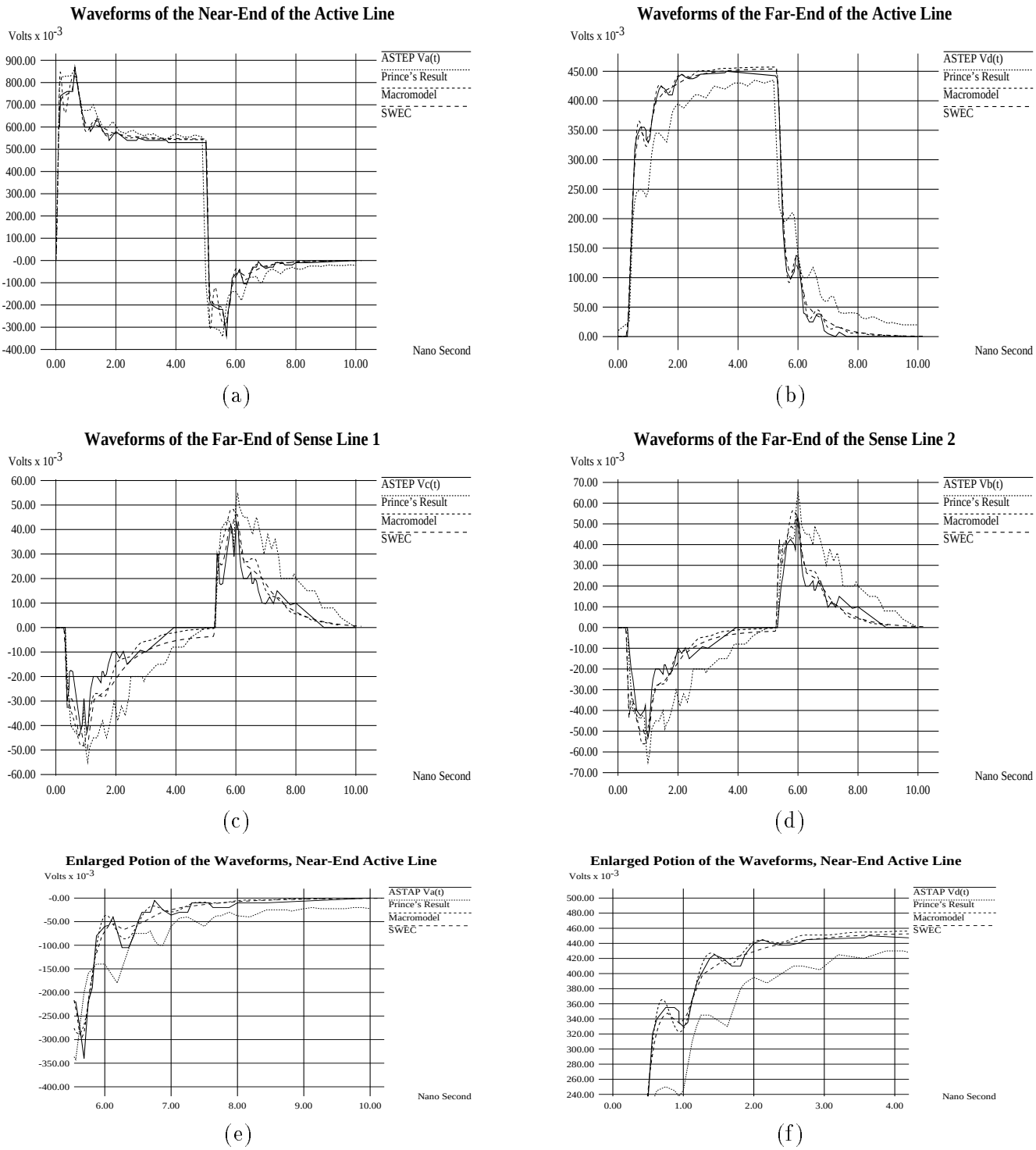

Figure 4.5: **Simulation Waveforms of the Two Groups of Three Coupled Lossless Transmission Lines:** The topology is shown in Figure 4.4. The output waveforms of the near end of the active line are shown in (a) together with its corresponding Cooke's, ASTAP and SWEC simulation results. The output waveforms of the far end of all three lines are shown in (b), (c), and (d) together with their corresponding Cooke's ASTAP and SWEC simulation results. Two enlarged portion of waveforms are shown in (e) and (f).

This has also been extended to the analysis of the coupled lossy transmission lines.

Taking full advantage of the frequency domain simulation nature of the scattering parameter based macromodel simulator, transient analysis of coupled transmission lines can approach the accuracy of SPICE-like simulator with orders of magnitude less computation time.

6 Acknowledgment

This work is supported in part by the National Science Foundation Presidential Young Investigator Award under the Grant MIP-9009945. Appreciations also goes to Ansoft Corporation for providing Maxwell/Spicelink software.

References

[1] M. Bayard. Synthesis of n-terminal pair networks. *Proc. Symposium on Modern Network Synthesis*, page 69, 1952. Eq. (7).

[2] F. Y. Chang. Transient analysis of lossless coupled transmission lines in a nonhomogeneous dielectric medium. *IEEE Trans. on Microwave Theory and Techniques*, MTT-18, No. 9:616–626, Sep. 1970.

[3] F.Y. Chang. The generalized method of characteristic for waveform relaxation analysis of lossy coupled transmission lines. *IEEE Trans. on Microwave Theory and Techniques*, MTT-37, No. 12:2028–2038, 1989.

[4] Eli Chiprout and M. Nakhla. Generalized moment-matching methods for transient analysis of interconnect networks. *9 th ACM/IEEE Design Automation Conference Proceedings*, pages 201–206, 1992.

[5] Eli Chiprout and Michel Nakhla. Transient waveform estimation of high-speed mcm networks using complex frequency hopping. In *Proc. of IEEE Multi-Chip Module Conference MCMC-93*, pages 0–0, 1993.

[6] Bradly J. Cooke, John Prince, and Andreas C. Cangellaris. S-parameter analysis of multiconductor, integrated circuit interconnect systems. *IEEE Trans. on Computer-Aided-Design*, 11, No. 3:353–360, 1992.

[7] Antonije. R. Djordjevic, Tapan. K. Sarkar, and Roger. F. Harrington. Time-domain response of multiconductor transmission lines. *Proceedings of the IEEE*, 75(6):111–132, 1987.

[8] J. Dobrowolski. *Introduction to Computer Methods for Microwave Circuit Analysis and Design.* Artech House, 1991.

[9] D. Hazony. *Elements of Network Synthesis.* Reinhold, New York, 1963.

[10] Haifang Liao and Wayne Dai. Extracting time-of-flight from scatering-parameter based macromodel. Technical Report 93-35, University of Clifornia, Santa Cruz, 1993.

[11] Haifang Liao, Wayne Dai, Rui Wang, and F. Y. Chang. Scatering-parameter based macro model of distributed-lumped networks using expnontially decayed polynomial function. In *Proc. of 30th ACM/IEEE Design Automation Conference*, pages 726–731, 1993.

[12] Haifang Liao, Rui Wang, Wayne Dai, and R. Chandra. Scatering-parameter based macro model of distributed-lumped networks using pade approximation. In *Proc. of International Symposium on Circuits and Systems*, 1993.

[13] Shen Lin, Marek-Sadowska M., and E. S. Kuh. Swec: a stepwise equivalent conductance timing simulator for cmos vlsi circuits. *EDAC. Proceedings of the European Conference on Design Automation*, pages 142–148, Feburary 1991.

[14] Fabio Romeo and Mauro Sanomauro. Time-domain simulation of n coupled transmission lines. *IEEE Trans. on Microwave Theory and Techniques*, MTT-35, No. 2:131–136, Feburary 1987.

[15] David S., Andrew T. Yang, and Sung Mo Kang. Modeling and simulation of interconnect delays and crosstalks in high-speed integrated circuits. *IEEE Trans. on Circuits and Systems*, Vol. 37:1–9, January 1990.

[16] Jose E. Schutt-Aine and Raj Mittra. Nonlinear transient analysis of coupled transmission lines. *IEEE Trans. on Microwave Theory and Techniques*, MTT-36, No. 7:959–966, 1989.